33RD INTERNATIONAL COSMIC RAY CONFERENCE, RIO DE JANEIRO 2013
THE ASTROPARTICLE PHYSICS CONFERENCE

ICRC 2013

Observations of the longitudinal development of extensive air showers with the surface detectors of the Pierre Auger Observatory

DIEGO GARCÍA-GÁMEZ[1] FOR THE PIERRE AUGER COLLABORATION[2]

[1] *Laboratoire de l'Accélérateur linéaire (LAL), Université Paris 11, CNRS-IN2P3, Orsay, France*
[2] *Full author list: http://www.auger.org/archive/authors_2013_05.html*

auger_spokespersons@fnal.gov

Abstract: Using the timing information from the FADC traces of surface detectors far from the shower core it is possible to reconstruct a Muon Production Depth distribution (MPD) to provide information about the longitudinal development of the muon component of Extensive Air Showers (EAS). We assess the quality of the MPD reconstruction for zenith angles around 60° and different energies of the primary particle. From these distributions we define $X^{\mu}_{\max}$, the depth, along the shower axis where the number of muons reaches maximum, and explore its potential as a useful observable to infer the mass composition of cosmic rays.

Keywords: Pierre Auger Observatory, ultra-high energy cosmic rays, muon production depth, mass composition

1 Introduction

Finding a solution to the question of the origin of the Ultra-High Energy Cosmic Ray (UHECR) requires three experimental feats: finding the mass of the primary particles, measuring the energy spectrum and detecting anisotropies in the distribution of their arrival directions. The energy spectrum is the best known of the three and its main features are well established [1, 2]. More controversial is whether the arrival directions of the highest-energy events are anisotropic [3, 4].

The situation regarding the mass composition of UHECRs is controversial. One way to determine the mass is to study the longitudinal development of the electromagnetic component of a shower. The depth of the shower maximum, $X_{\max}$, is sensitive to the nature of the primary [5]. However $X_{\max}$ measurements suffer from low statistics due to the small duty cycle of the fluorescence detectors and the stringent cuts imposed to avoid a biased data sample [6].

The Auger Collaboration has proposed different methods [7] to infer masses that take advantage of the large statistical sample provided by the high-duty cycle of the surface detector (SD) array. Here we describe one of them. It relies on the study of the longitudinal development of the muonic component of EAS. The surface detectors of the Observatory provide this information through the timing records associated with the muons that reach ground. The muon arrival-times allow the reconstruction of their production points along the shower axis. It is thus possible to reconstruct a distribution of Muon Production Depths [8]. Since muons come from the decay of pions and kaons, the shape of the MPD contains information about the evolution of the hadronic cascade. This information renders interesting the study of MPDs for the following reason: we know that different primaries have distinct hadronic properties (i.e. cross-section and multiplicity) that translate into variations of their respective longitudinal profiles. Therefore it is natural to think that the shape of the MPD must be sensitive to the mass of primary particle.

2 The Model for the Muon Arrival Time Distributions

Muons reaching ground have a time structure caused by the importance of different mechanisms during muon propagation. Through a set of simple assumptions, those arrival times can be used to obtain the distribution of muon production distances along the shower axis. The basis of our measurement is a theoretical framework originally developed in [9, 10] and updated in [11]. As a first approximation we assume that muons travel in straight lines at the speed of light c and neglect the delay accumulated by the parent mesons. Muons produced at the position z (along the shower axis) that reach ground at the point defined by (r,ζ) have travelled a distance l given by the expression:

$$l = ct_{\mu} = \sqrt{r^2 + (z-\Delta)^2} \tag{1}$$

where t_{μ} is the muon time of flight. r and ζ are measured in the shower reference frame and represent the distance and the azimuthal position of the point at ground respectively. $\Delta = r\tan\theta\cos\zeta$ is the distance from the point at ground to the shower plane. If we reference the muon time of flight to the arrival time of the shower-front plane for each position (r,ζ), we obtain the *geometrical delay* t_g:

$$ct_g = \sqrt{r^2 + (z-\Delta)^2} - (z-\Delta). \tag{2}$$

Therefore there is a one-to-one correspondence between measured arrival times and muon production distances. The actual muon delay includes effects related to the fact that muon velocities are subluminal (causing a *kinematical delay* t_{ε}). Delays produced by the geomagnetic field and multiple scattering are of lesser importance [11]. The muon production point along the shower axis z is given by the expression:

$$z \simeq \frac{1}{2}\left(\frac{r^2}{ct - c<t_{\varepsilon}>} - (ct - c<t_{\varepsilon}>)\right) + \Delta \tag{3}$$

where the geometrical delay t_g has been approximated by $t_g \simeq t - <t_{\varepsilon}>$.

3 Reconstruction of Muon Production Depth

The MPD is reconstructed from the FADC signals from the water-Cherenkov detectors. The production depth X^{μ} comes from an integration of the atmospheric density, ρ, over the range of production distances:

$$X^{\mu} = \int_{z}^{\infty} \rho(z')dz'. \quad (4)$$

The shape of the distribution depends strongly on the observation point at ground as the surface detectors sample the particle cascade at different stages of its development. For discrete detector arrays just a handful of r values are available. This implies that in general the measured MPD will show a severe distortion when compared to the true MPD shape. The MPD observed at ground also depends on the zenith angle. This is mainly a consequence of the muon decay probability. It influences not only the location of the maximum but also shapes the observed MPD.

To gain insight to the physics from the reconstructed shape of the MPD, a fit is made using the Gaisser-Hillas function. Of its four parameters, the one referred to as $X^{\mu}_{\rm max}$ accounts for the point along the shower axis where the production of muons reaches a maximum. As shown later, this parameter will be our main physics observable for composition studies. The MPD fit is performed in an interval of depths ranging from 0 to 1200 g cm^{-2} that contains the entire range of possible values of $X^{\mu}_{\rm max}$ (our deepest simulated proton shower has an $X^{\mu}_{\rm max} \sim 1000$ g cm^{-2}). Simulations show that the $X^{\mu}_{\rm max}$ distribution varies as a function of the mass of the primary particle. For heavier primaries, the average value of $X^{\mu}_{\rm max}$ is smaller and the distribution narrower compared with that for lighter particles (Figure 1). This behaviour is independent of the energy of the primary cosmic ray. The signals registered by the surface detectors are from a mix of muons and electromagnetic (EM) particles. To build the MPD of an event we are only concerned with the behaviour of the muonic component. The EM signal is a background that must be eliminated. One way to do this is to use inclined events ($\theta >\sim 60^{\circ}$). For these data, the EM component is heavily absorbed by the atmosphere. Inclined events are also of special interest for this analysis since the dependence of the MPD shape with the distance to the shower axis r drastically decreases as θ increases. This helps to reduce the impact that the spacing of the Auger surface detectors have in the reconstruction of $X^{\mu}_{\rm max}$. Therefore, for the sake of simplicity, the present work focuses only on data for which the zenith angles lie in the interval $[55^{\circ}, 65^{\circ}]$.

The EM contamination can be further reduced by exploiting the different behaviors of the EM and muonic components. In general, the EM signals are smaller and broader. As a consequence, a cut on signal threshold that rejects all time bins with signals below a certain value ($S_{threshold}$) will help diminish the EM contamination.

To build the production depth distribution, every time bin of the FADC traces is converted to an entry in it by means of equation 3. Since the typical time stamp of a muon does not fall into a single time bin but it rather spans several bins with a known, gamma-like, distribution, we have an uncertainty in the arrival time of muons that must be accounted for. To compensate for this detector effect, we subtract an offset T_{shift}. It depends on $S_{threshold}$ and hence simulations must be used to find an appropriate value. Requiring that for $S_{threshold}$= 0.4 VEM the reconstruction of our lower energy events is unbiased, we find T_{shift}= 70 ns. We use this value throughout the range of interest. To guarantee that the reconstruction bias in $X^{\mu}_{\rm max}$ lies within $\pm$10 g cm^{-2} for all energies, $S_{threshold}$ is increased slowly with energy, reaching a maximum value of 0.6 when dealing with the most energetic events.

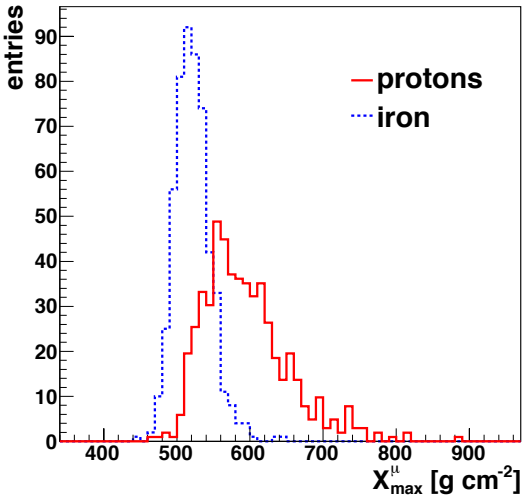

Figure 1: $X^{\mu}_{\rm max}$ distributions for proton and iron showers simulated at 30 EeV with Epos-LHC [12] at zenith angles between 55° and 65°. The mean value and the RMS of the distributions show a clear dependence upon the mass of the primary cosmic ray. For the construction of these MPDs, only muons reaching ground at distances greater than 1700 m have been considered.

For each time bin, the uncertainty introduced in X^{μ} (δX^{μ}) is a function of the FADC sampling rate (δt) and the accuracy of reconstruction of the shower angle and core location. The sampling frequency is 40 MHz, and gives rise to an uncertainty in the z reconstruction [9, 10] , that decreases quadratically with r, and increases linearly with z as:

$$\frac{\delta z}{z} \simeq 2\frac{z}{r^2}c\delta t. \quad (5)$$

It is evident that the closer we get to the impact point at ground, the larger the uncertainty in z (and in X^{μ} through equation 4). The contribution of the geometrical reconstruction to δX^{μ} also increases as we get closer to the core. Thus, to keep the distortions of the reconstructed MPD small, only surface detectors far from the core are useful. A cut in core distance, r_{cut}, is therefore mandatory. This cut diminishes the efficiency of the reconstruction and also affects the resolution as it reduces the number of muons in the reconstruction: note that the total uncertainty of the MPD maximum, $\delta X^{\mu}_{\rm max}$, depends on the number of muons N_{μ}, and therefore decreases as the square root of N_{μ}. The reconstruction efficiency however improves with energy, as the number of muons becomes larger as energy increases. As the number of muons at ground is a function of the mass of the primary, we risk introducing a bias in our selection towards heavier nuclei if the value for r_{cut}

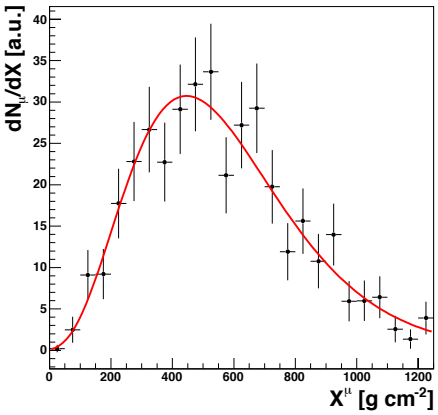

Figure 2: Real reconstructed MPD, θ = (59.06 $\pm$ 0.08)° and E = (92 $\pm$ 3) EeV, with the fit to a Gaisser-Hillas function.

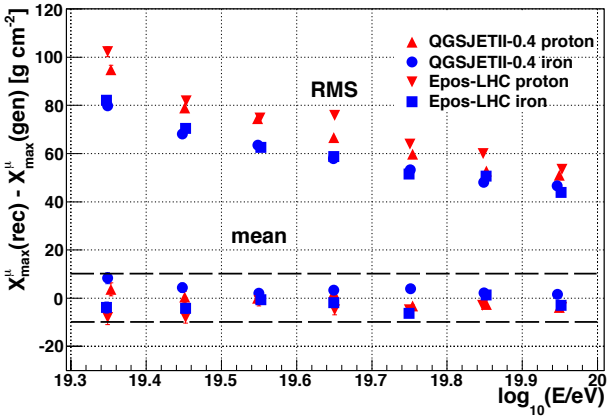

Figure 3: Evolution with energy of the RMS of the distribution [$X^{\mu}_{\rm max}$ (reconstructed) - $X^{\mu}_{\rm max}$ (true)]. The simulations were made using the QGSJETII-0.4 [13] and EPOS-LHC hadronic models for proton and iron nuclei for 55 ° $\leq \theta \leq$ 65°.

is not carefully chosen. Therefore the selection of the distance cut must be a trade off between the resolution of the reconstructed MPD and the number of muons being accepted into such reconstruction [8]. We use Monte Carlo simulations to choose the optimal value for r_{cut}. To build the MPD, we consider only those detectors whose distance to the shower core is larger than 1700 m, regardless of the shower energy. Choosing an r_{cut} which is independent of energy implies that any difference in resolution that we find for different energies will be a consequence mainly of the different number of muons detected at ground. To estimate the impact that the distance cut and the undersampling in r have on the determination of $X^{\mu}_{\rm max}$, we have studied the variation of $X^{\mu}_{\rm max}$ as a function of r_{max} (upper limit of the distance interval [r_{cut}, r_{max}] used to integrate the MPD). Our simulations show that the variation of the $X^{\mu}_{\rm max}$ value amounts to about 10 g cm^{-2} per km shift in r_{max}.

The fact that in the selected data we do not use triggered stations further than ~4000 m implies that we build MPDs by counting muons at ground in the distance range 1700 m $\leq$ r $\leq$ 4000 m. The MPD for a single detector is obtained as the average of the three MPDs that each PMT yields. For each event, the final MPD is obtained by adding the individual MPDs observed by each of the selected surface detectors. Figure 2 shows the reconstructed MPD for one of our most energetic events.

We select longitudinal profiles measured using a simple set of criteria: a) **Trigger cut.** We select EAS that fulfill a T5 trigger condition which requires that the detector with the highest signal has all 6 closest neighbours operating; b) **Energy cut.** We restrict our analysis to events with energy larger than 20 EeV as for the less energetic events the population of the MPD is very small, giving a very poor determination of $X^{\mu}_{\rm max}$; c) $\mathbf{X^{\mu}_{max}}$ **error.** We reject events whose relative error in $X^{\mu}_{\rm max}$ is bigger than a certain value $\varepsilon_{\rm max}$, an energy-dependent quantity (see Table 1) since the accuracy in the estimation of $X^{\mu}_{\rm max}$ improves with energy. This is a natural consequence of the increase in the number of muons that enter the MPD as the energy grows.

The event selection efficiencies after the cut in $X^{\mu}_{\rm max}$ uncertainty (cut c) are greater than 80%. Monte Carlo studies have shown that the cuts chosen introduce a composition bias smaller than 2 g cm^{-2} (included as a systematic uncertainty). Also, as shown in Figure 3, the absolute value of the mean bias in reconstructions is $<$ 10 g cm^{-2}, regardless of the hadronic model, energy and atomic mass of the simulated primary. The resolution, understood as the RMS of the distribution [$X^{\mu}_{\rm max}$ (reconstructed) - $X^{\mu}_{\rm max}$ (true)], ranges from 100 (80) g cm^{-2} for proton (iron) at the lower energies to about 50 g cm^{-2} at the highest energy (see Figure 3). The improvement of the resolution with energy is a direct consequence of the increase in the number of muons.

$\log_{10}$E/eV	$\varepsilon_{\rm max}$(%)
[19.3, 19.4]	15
[19.4, 19.6]	11
[19.6, 19.7]	10
[19.7, 19.8]	8
$>$ 19.8	7

Table 1: Maximum relative errors allowed in the estimation of $X^{\mu}_{\rm max}$. The value chosen for $\varepsilon_{\rm max}$ ensures no selection bias between the different primary species.

4 Application to data

The data set used in this analysis comprises the events recorded from 1-January 2004 to 31-December 2012. We compute MPDs on an event-by-event basis. We have shown that for events with zenith angles in the interval 55° $\leq \theta \leq$ 65°, the total MPD is simply the direct sum of the individual MPDs given by the set of selected water-Cherenkov detector traces. For this angular range, our initial sample is therefore made of 663 events.

To guarantee an accurate reconstruction of the longitudinal profile we impose the selection criteria described in Section 3. Table 2 summarises how the different cuts reduce the number of events.

The evolution of the measured $\langle X^{\mu}_{\rm max} \rangle$ as a function of energy is shown in Figure 4. The data have been grouped in five energy bins of width 0.1 in $\log_{10}$(E/eV), except

Cut	Events	Efficiency (%)
$55° \leq \theta \leq 65°$, E>20 EeV	663	100
T5 trigger*	500	75
$\varepsilon(X^{\mu}_{\rm max})<\varepsilon_{\rm max}$	481	73

Table 2: Selection procedure applied to the SD data. * Described in Section 3.

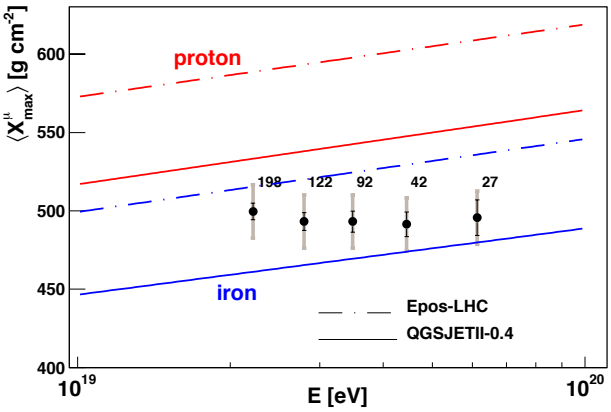

Figure 4: $\langle X^{\mu}_{\rm max} \rangle$ as a function of energy. The prediction of different hadronic models for proton and iron are shown. Numbers indicate the amount of selected data in each energy bin and the gray rectangles represent the systematic uncertainty.

for the last which contains all events with energy above $\log_{10}$(E/eV)=19.7 (50 EeV). The uncertainties represent the standard error on the mean.

Table 3 lists the most relevant sources contributing to the systematic uncertainty. The uncertainties on the MPD reconstruction and event selection translate into an overall systematic uncertainty on $\langle X^{\mu}_{\rm max} \rangle$ of 17 g cm^{-2}.

The interpretation of data in terms of mass composition requires a comparison with air shower simulations. For models like those of Figure 4 that assume standard hadronic interactions, the evolution of the mean $X^{\mu}_{\rm max}$ values may suggest a change in composition as the energy increases (flatter trend than pure proton or pure iron predictions). However as the MPD technique currently suffers from small statistics and large resolution measurements, a constant composition would also be acceptable. At this stage, we cannot make conclusive inferences about mass composition. The proposed method can also be used as a tool to investigate the validity of hadronic interaction models. In Figure 4 we can see how QGSJETII-0.4 and EPOS-LHC predict, for both proton and iron, the same *muonic elongation rate* (rate of evolution of $X^{\mu}_{\rm max}$ with energy) but with considerable differences in the absolute value of $X^{\mu}_{\rm max}$. The measurement of muon profiles provides complementary data that set additional constraints to model descriptions and improves understanding of hadronic interactions.

5 Conclusions

The FADC traces from the water-Cherenkov detectors at the Auger Observatory located far from the core have been used to make reconstructions of the muon production depth distributions on an event-by-event basis. The maximum of the distribution $X^{\mu}_{\rm max}$ contains information about the mass composition of UHECR. It can be used also to assess the validity of hadronic interaction models at ultra-high energies. With this analysis we have established a novel approach to study the longitudinal development of the hadronic component of EAS.

Source	Sys. Uncertainty (g cm^{-2})
Reconstruction + hadronic model + primary	10
Core time	5
Atmospheric profile	8
Fitting procedure	3
Selection efficiency	2
Energy uncertainties	3
Seasonal	8
Total	17

Table 3: Evaluation of the main sources of systematic uncertainties.

Acknowledgment: D. Garcia Gamez was supported by the ANR-2010-COSI-002 grant of the French National Research Agency.

References

[1] R. U. Abbasi *et al.*, Astropart. Phys. **32** (2009) 53
[2] The Pierre Auger Collaboration, Phys. Lett. B **685** (2010) 239
[3] The Pierre Auger Collaboration, Astropart. Phys. **34** (2010) 314
[4] R. U. Abbasi *et al.*, Astropart. Phys. **30** (2008) 175
[5] R. M. Baltrusaitis, for the Flys Eye Collaboration, Proc. 19th ICRC, La Joya, USA, **30** (1985) 166
[6] V. de Souza, for the Pierre Auger Collaboration, paper 0751, these proceedings
[7] D. Garcia-Pinto, for the Pierre Auger Collaboration, Proc. 32nd ICRC, Beijing, China, **2** (2011) 87, arXiv:1107.4804 [astro-ph]
[8] D. Garcia-Gamez, PhD Thesis, `http://cafpe10.ugr.es/cafpe_new/tesis/Tesis_DGarcia.pdf`
[9] L. Cazon, R. A. Vazquez, A. A. Watson and E. Zas, Astropart. Phys. **21** (2004) 71
[10] L. Cazon, R. A. Vazquez and E. Zas, Astropart. Phys. **23** (2005) 393
[11] L. Cazon, R. Conceição, M. Pimenta, E. Santos Astropart. Phys. **36** (2012) 211
[12] T. Pierog, talk at the Recontres de Moriond, March 2013. To be published in the Proceedings.
[13] S. Ostapchenko, Phys. Lett. B **703** (2011) 588